

SOURCE LOCALIZATION OF EEG/MEG DATA BY CORRELATING COLUMNS OF ICA SOLUTION WITH LEAD FIELD MATRIX

Kenneth E. Hild II, Srikantan S. Nagarajan

Department of Radiology
University of California at San Francisco, CA, USA
k.hild@ieee.org, sri.nagarajan@radiology.ucsf.edu

ABSTRACT

Independent Components Analysis is increasingly being used on EEG/MEG data as a preprocessor to source localization methods such as beamforming and dipole fitting. Here we show how ICA can be used to perform source localization directly. The proposed method consists of dimension reduction preprocessing, estimating and inverting the reduced-dimension demixing matrix, and then correlating the columns of the resulting mixing matrix estimate with the columns of the forward model. The results section shows a comparison of the proposed method and a scalar minimum variance beamformer, where it is shown that the proposed ICA-based method has less localization error.

Index Terms— Biomedical electromagnetic imaging, Electroencephalography, Separation

1. INTRODUCTION

Since its inception in the late 1980's Independent Components Analysis (ICA) has been used for a variety of applications. The list of applications includes blind source separation (BSS) [1], identification, angle of arrival estimation, deconvolution, preprocessing for feature extraction, and denoising/artifact rejection. Unlike for many of the applications in this list, reasonable estimates of the forward (mixing) model is known or can be estimated for applications involving electroencephalographic (EEG) and magnetoencephalographic (MEG) data. The forward model, which is a function of the composite lead field matrix, can be used for estimating the spatial locations of each source. It is becoming commonplace to use ICA preprocessing on EEG and MEG data in an attempt to directly extract meaningful components, such as evoked responses, or to remove unwanted interference, such as cardiac artifacts. The ICA preprocessing is performed in hopes of improving the subsequent source localization. Instead of using ICA as a preprocessor, we show how source localization can be directly performed using the ICA solution and the composite lead field matrix.

2. SOURCE LOCALIZATION

For MEG data, if we assume a homogeneous spherical conductor model, the ($M \geq 1$) measured magnetic field at time n is given by,

$$\mathbf{b}_n = \mathbf{L}_c \Psi \begin{bmatrix} \mathbf{s}_n \\ \mathbf{x}_n \end{bmatrix} + \mathbf{B} \mathbf{y}_n + \boldsymbol{\eta}_n \quad (1)$$

where \mathbf{L}_c is the ($M \geq D Q_{sx}$) composite lead field matrix (defined below), Ψ is the ($D Q_{sx} \geq Q_{sx}$) orientation matrix, \mathbf{s}_n is the ($Q_s \geq 1$) vector of neural sources of interest (hereafter referred to as neural sources), \mathbf{x}_n is the ($Q_x \geq 1$) vector of neural sources of no interest (hereafter referred to as neural interference), \mathbf{B} is a ($M \geq Q_y$) transfer function matrix, \mathbf{y}_n is the ($Q_y \geq 1$) vector of non-neural interference, the term “source” is used for either a neural source, a neural interference, or a non-neural interference as determined by context, $\boldsymbol{\eta}_n$ represents the noise and model error, and where M is the number of sensors, D equals the rank of $\mathbf{L}_c \Psi \Psi^T \mathbf{L}_c^T$ (3 in general, but 2 for our assumptions), and $Q_{sx} = Q_s + Q_x$ is the number of neural sources/interference. Due to the structure of the orientation matrix the product of \mathbf{L}_c and Ψ can be expressed as,

$$\mathbf{L}_c \Psi = [\mathbf{L}_1 \boldsymbol{\eta}_1 \quad \mathbf{L}_2 \boldsymbol{\eta}_2 \quad \dots \quad \mathbf{L}_{Q_{sx}} \boldsymbol{\eta}_{Q_{sx}}] \quad (2)$$

where each ($M \geq D$) lead field matrix \mathbf{L}_i represents the transfer function from any specified spatial location to the sensors (the elements of which depend only on the spatial location of source i relative to the sensor locations) and each ($D \geq 1$) vector $\boldsymbol{\eta}_i$ represents the orientation of source i . The same model also holds for EEG data (although the lead field matrices differ for MEG and EEG data).

The lead field matrices are known, whereas the orientation matrix must be estimated from the data. Notice that (1) implicitly requires knowledge of the source locations. Although the lead field matrices are known for any spatial location, it is not known a priori which spatial locations correspond to the Q_{sx} sources. One way to perform source localization is to create a dense grid of $\bar{Q}_{sx} \gg Q_{sx}$ potential source locations and then to scan each potential source location. The spatially

oversampled data can be expressed as,

$$\mathbf{b}_n = \mathbf{L}_c \mathbf{\Psi} \begin{bmatrix} \mathbf{\Psi}_i \\ \mathbf{\Psi}_n \end{bmatrix} + \mathbf{B} \mathbf{y}_n + \boldsymbol{\eta}_n \quad (3)$$

where \mathbf{L}_c is a $(M \geq D\bar{Q}_{sx})$ matrix, $\mathbf{\Psi}$ is a $(D\bar{Q}_{sx} \geq \bar{Q}_{sx})$ matrix, $\mathbf{\Psi}_i$ is a $(\bar{Q}_s \geq 1)$ vector, $\mathbf{\Psi}_n$ is a $(\bar{Q}_x \geq 1)$ vector, $\bar{Q}_{sx} = \bar{Q}_s + \bar{Q}_x$, and where $\bar{Q}_s \geq Q_s$ elements of $\mathbf{\Psi}_i$ and $\bar{Q}_x \geq Q_x$ elements of $\mathbf{\Psi}_n$ have zero power. The dimensions of \mathbf{B} and \mathbf{y}_n do not change since the forward model for non-neural sources is unknown. In beamforming the orientation vector is estimated at each voxel and then the power of the source at that location is estimated. Dipole fitting can also be thought of in this manner with the primary exception that beamforming considers each voxel separately, whereas dipole fitting considers the voxels simultaneously. Hence, source localizations using beamforming generally have non-zero power at all \bar{Q}_{sx} voxels (ideally, for beamforming, most of the energy is concentrated in Q_{sx} locations in source space), whereas dipole fitting has non-zero power at only Q_{sx} voxels.

3. PROPOSED METHOD FOR SOURCE LOCALIZATION

The proposed method is based on a BSS solution. Using BSS terminology the matrix $[\mathbf{L}_c \mathbf{\Psi} \mathbf{B}]$ is known as the mixing matrix, which we denote as \mathbf{A} , and the concatenation of the neural sources, neural interference, and non-neural interference is known as the source vector, which we denote as \mathbf{u}_n (which is assumed to have zero mean). Hence, the data can be expressed as,

$$\mathbf{b}_n = \mathbf{A} \mathbf{u}_n + \boldsymbol{\eta}_n \quad (4)$$

where \mathbf{A} is size $(M \geq Q)$ and $Q = Q_s + Q_x + Q_y$. Likewise, the source estimates are given by,

$$\hat{\mathbf{u}}_n = \mathbf{W}_2 \mathbf{W}_1 \mathbf{b}_n \quad (5)$$

where \mathbf{W}_1 is a $(\hat{Q} \geq M)$ projection matrix found using any desired dimension-reduction method and \mathbf{W}_2 is a full-rank $(\hat{Q} \geq \hat{Q})$ matrix found using any desired BSS algorithm (here we use ICA to perform separation).

To simplify the explication we will temporarily assume that there is no noise and that we know Q . We also make several usual assumptions, e.g., the mixing is linear and memoryless, there are at least as many sensors as sources $(M \geq Q)$, and the sources are mutually statistically-independent and non-Gaussian. In this case it is well-known that perfect estimation of both \mathbf{u}_n and \mathbf{A} (up to an arbitrary scaling and permutation) occurs when the columns of \mathbf{W}_1 are the eigenvectors of $E[\mathbf{b}_n \mathbf{b}_n^T]$ having non-zero eigenvalues and \mathbf{W}_2 is such that the source estimates are statistically independent. The estimate of \mathbf{A} is found using the pseudo-inverse of $\mathbf{W}_2 \mathbf{W}_1$,

which takes the form,

$$\begin{aligned} \hat{\mathbf{A}} &= (\mathbf{W}_2 \mathbf{W}_1)^\dagger \triangleq \mathbf{W}_1^T \mathbf{W}_2^T (\mathbf{W}_2 \mathbf{W}_1 \mathbf{W}_1^T \mathbf{W}_2^T)^{*1} \\ &= \mathbf{W}_1^T \mathbf{W}_2^T \mathbf{W}_2^* T (\mathbf{W}_1 \mathbf{W}_1^T)^{*1} \mathbf{W}_2^{*1} \quad (6) \\ &= \mathbf{W}_1^T \mathbf{W}_2^{*1} \end{aligned}$$

since the columns of \mathbf{W}_1 are ortho-normal and \mathbf{W}_2 is invertible. Due to the indeterminacies of BSS the pseudo-inverse of $\mathbf{W}_2 \mathbf{W}_1$ at the separating solution equals \mathbf{DPA} , where \mathbf{D} is a diagonal matrix and \mathbf{P} is a permutation matrix. As discussed below knowledge of \mathbf{DPA} is sufficient to perform neural source localization using the proposed method.

The proposed column correlation method involves two steps. First, we estimate the orientation vector at each voxel. Second, for each voxel we express our level of confidence that a source resides at that voxel. The confidence level for voxel j is determined using the following similarity metric,

$$\begin{aligned} \rho_j &= \max_i \rho_{ij} \\ \rho_{ij} &= \frac{|\hat{\mathbf{A}}_i^T \boldsymbol{\Psi}_j|}{\left(\hat{\mathbf{A}}_i^T \hat{\mathbf{A}}_i \boldsymbol{\Psi}_j^T \boldsymbol{\Psi}_j\right)^{1/2}} \quad (7) \end{aligned}$$

where $\hat{\mathbf{A}}_i$ is the i^{th} column of $\hat{\mathbf{A}}$ and $\boldsymbol{\Psi}_j$ is the j^{th} column of $\mathbf{L}_c \mathbf{\Psi}$. This approach implicitly assumes that there is a source at every voxel thus allowing for the possibility that the proposed method can describe distributed sources (two or more point sources having the same time course). The proposed method is similar to beamforming in this respect.

The orientation of voxel j is chosen as the orientation that maximizes (7). This can be written as,

$$\begin{aligned} \boldsymbol{\eta}_j^* &= \max_{\boldsymbol{\eta}_j} \frac{|\hat{\mathbf{A}}_i^T \boldsymbol{\Psi}_j|}{\left(\hat{\mathbf{A}}_i^T \hat{\mathbf{A}}_i \boldsymbol{\Psi}_j^T \boldsymbol{\Psi}_j\right)^{1/2}} \\ &= \max_{\boldsymbol{\eta}_j} \frac{\boldsymbol{\Psi}_j^T \hat{\mathbf{A}}_i \hat{\mathbf{A}}_i^T \boldsymbol{\Psi}_j}{\boldsymbol{\Psi}_j^T \boldsymbol{\Psi}_j} \quad (8) \\ &= \max_{\boldsymbol{\eta}_j} \frac{\boldsymbol{\eta}_j^T \mathbf{L}_j^T \hat{\mathbf{A}}_i \hat{\mathbf{A}}_i^T \mathbf{L}_j \boldsymbol{\eta}_j}{\boldsymbol{\eta}_j^T \mathbf{L}_j^T \mathbf{L}_j \boldsymbol{\eta}_j} \end{aligned}$$

since (7) is non-negative, $\hat{\mathbf{A}}_i^T \hat{\mathbf{A}}_i$ is a positive scalar (which does not effect maximization), and by substituting $\mathbf{L}_j \boldsymbol{\eta}_j$ for $\boldsymbol{\Psi}_j$. Notice that both $\mathbf{L}_j^T \hat{\mathbf{A}}_i \hat{\mathbf{A}}_i^T \mathbf{L}_j$ and $\mathbf{L}_j^T \mathbf{L}_j$ are symmetric and positive semi-definite matrices. Hence, the vector $\boldsymbol{\eta}_j$ that maximizes (8) is given by the eigenvector associated with the largest eigenvalue of the generalized eigenvalue decomposition (GED) of $\mathbf{L}_j^T \hat{\mathbf{A}}_i \hat{\mathbf{A}}_i^T \mathbf{L}_j$ and $\mathbf{L}_j^T \mathbf{L}_j$. The maximum operator causes the map to be segmented into Q_s mutually exclusive and collectively exhaustive regions (not shown here due to space restrictions). This is unlike dipole fitting, which

selects exactly Q_s points of activity on the map and assumes the remaining voxels are inactive. We also tried, in place of the maximization operation, taking the mean over i and a weighted mean over i (where the weight is given by the mean power of the i^{th} source measured in sensor space). We chose to maximize over i since it performs better in empirical tests.

Knowledge of *DPA* is sufficient to perform neural source localization as long as the matrix $\mathcal{P}_c\Psi$ is full-column rank and it includes the true (neural) source locations, which becomes more likely as \bar{Q} increases. Recall that each column of $\mathcal{P}_c\Psi$ corresponds to a single, known spatial location. With the assumptions above each column of \mathcal{A} should be proportional to one of the columns of either $\mathcal{P}_c\Psi$ or \mathcal{B} , the latter of which can be ignored for neural localization since it represents non-neural activity. Since the order of the columns in (7) is irrelevant the \mathcal{P} matrix can be ignored. The \mathcal{D} matrix can also be ignored since (7) does not depend on the norm of either column, which is the reason we chose the (absolute) normalized correlation coefficient for the similarity metric. Notice that the proposed method can be made to be similar to dipole fitting by selecting for each column i the single voxel j that maximizes (7).

The lead field matrices are often highly correlated so the resulting map lacks sharp peaks. Hence, for visualization purposes we suggest subtracting the minimum value of ρ_j and then dividing by the maximum value, so that the map takes values between 0 and 1, and then raising the result to a value greater than 1. We choose the exponent as the minimum value required to ensure that less than 2% of the map has an exponentiated correlation larger than 25% of the maximum exponentiated correlation. This has no effect on the locations of the peaks, but it does change the relative heights of the peaks.

The interference needs to be suppressed since we are only interested in localizing s_n . Likewise, we do not wish for the noise to negatively effect the localization. The proposed method is robust with respect to non-neural interference whenever the columns of \mathcal{B} are nearly orthogonal to the columns of $\mathcal{P}_c\Psi$, as can be seen from (7) whenever a column of $\hat{\mathcal{A}}$ is proportional one of the columns of \mathcal{B} . Likewise, it is robust with respect to noise whenever the columns of an identity matrix and the columns of $\mathcal{P}_c\Psi$ are nearly orthogonal. Additional suppression is obtained by properly selecting the \mathcal{W}_1 projection matrix. If the (neural) signal-to-noise+interference ratio (SNIR) is large or if the noise and interference are spatially uncorrelated and isotropic then PCA is a good choice for learning \mathcal{W}_1 . Here we assume the data is collected using the stimulus-evoked paradigm so that we can use PFA [2] to find an appropriate projection. PFA is able to suppress the neural and non-neural interference and noise whether or not the SNIR is large or the noise and interference are spatially uncorrelated and isotropic.

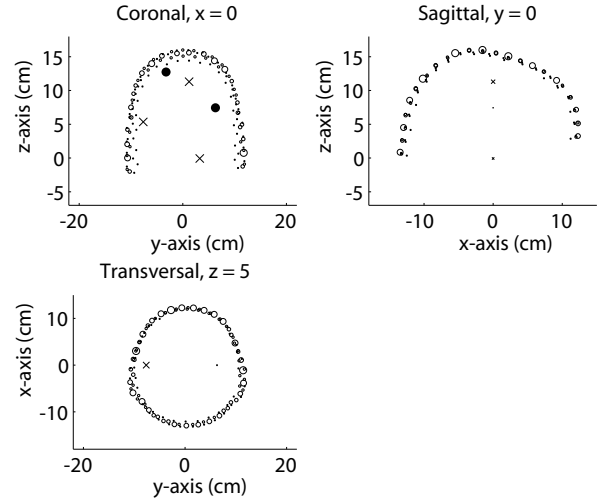


Fig. 1. Locations of the 2 sources (\bullet), the 3 interferences (\times), and the 275 sensors (O) for a single Monte Carlo trial.

4. RESULTS

We use a total of 250 different synthetically generated evoked-response datasets, which correspond to 50 Monte Carlo trials for each of 5 different values of (neural) signal-to-interference ratio (SIR). Each dataset is 1000 samples in length, 5/8 of which corresponds to the pre-stimulus period and 3/8 to the post-stimulus period, and the sampling frequency is 1 kHz. Each neural source has a damped sinusoidal time course having a random frequency between 5-20 Hz, whereas each neural interference has an un-damped sinusoidal time course. Damping is performed such that the energy of the neural sources is concentrated within the post-stimulus period. The number of sensors is $M = 275$, the number of neural sources, neural interferences, and non-neural interferences is $Q_s = 2$, $Q_x = 3$, $Q_y = 0$, respectively. Figure 1 shows the locations of the neural sources, neural interference, and sensors for one trial. The size of each marker indicates how close the corresponding source/interference/sensor is to the plane in question. Additive (spatially and temporally) white Gaussian noise is added to each sensor. The power of the (isotropic) noise relative to the power of the neural sources is -5 dB. The power of the neural interference relative to the power of the neural sources (SIR) is varied from -10 dB to 10 dB in 5 dB increments.

Determination of the lead field matrices requires knowledge of the spatial locations of the sensors. For this we use the true spatial locations of the sensors corresponding to an in-house 275-channel whole head MEG system (Omega 2000, VSM MedTech Inc., Port Coquitlam, Canada). For simplicity the spatial locations of the neural sources and the neural interferences all lie within the $x = 0$ transversal plane.

We use a scalar minimum variance beamformer [3], which

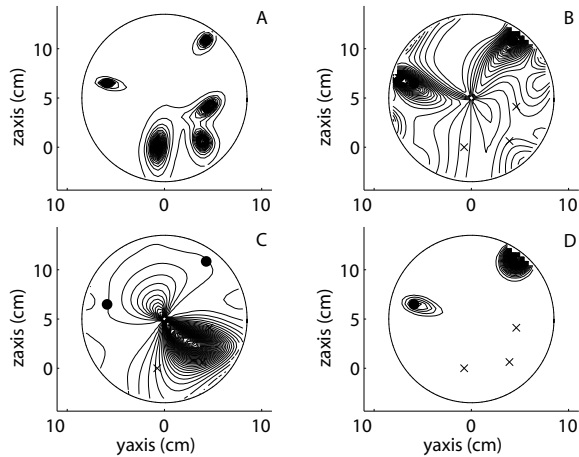


Fig. 2. Contour plots of the tomographic maps for a single Monte Carlo trial. A) Raw Data/Beamformer, B) PFA/Beamformer, C) PCA/Beamformer, and D) PFA/Column Correlation. The \circ 's and \times 's correspond to the true neural source and interference locations, respectively.

requires inversion of the appropriate covariance matrix. The data covariance matrix is used if denoising is not applied and the denoised data covariance matrix is used otherwise. Bayesian regularization is used for inverting ill-conditioned matrices. Beamforming is used on the raw data as well as with the data after PCA and PFA denoising are applied. Both PCA and PFA assume that there are 2 neural sources.

The performance is measured using the localization error, which is the mean distance between the true neural source locations and the estimated locations. The estimated locations correspond to the largest two peaks of the tomographic map. Since there are 2 neural sources, there are two different ways of associating the true source locations with the estimated source locations. We use the more meaningful association, which is the one that has a smaller mean distance.

Figure 2 shows contour plots for the beamformer reconstruction when it is used with the raw data and with PCA and PFA denoised data. Also shown is the proposed method for source localization (combined with PFA). Notice that, for this example, the Raw Data/Beamformer finds all 5 neural sources/interference, the PCA/Beamformer map is indistinct, and the PFA/Column Correlation and PFA/Beamformer maps find the two neural sources.

Figure 3 shows the mean localization error as a function of the input SIR. PCA/Beamformer consistently performs the worst, PFA/Column Correlation consistently outperforms the PFA/Beamformer and PCA/Beamformer, and the Raw Data/Beamformer performs poorly for low SIR and performs the best (as expected) for high SIR.

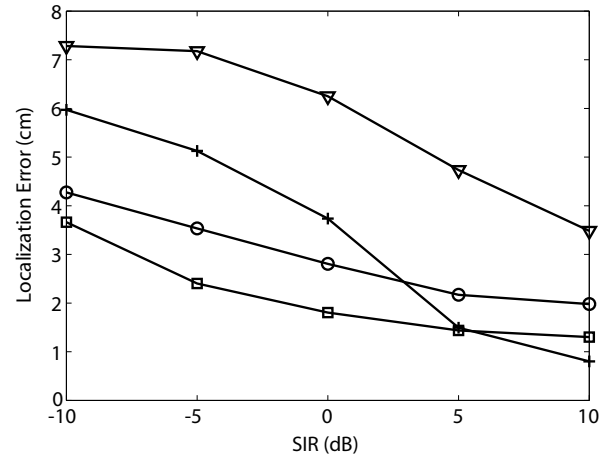


Fig. 3. Mean localization error over all 50 Monte Carlo trials as a function of input SIR. Results are shown for Raw Data/Beamformer (+), PFA/Beamformer (O), PCA/Beamformer (∇), and PFA/Column Correlation (\square). Bayesian regularization is used whenever required.

5. DISCUSSION

The proposed method requires the inversion of a Q_s -dimensional matrix (2 in our example) as opposed to the three beamformer implementations, which require the inversion of an M -dimensional matrix (275 in our example). The proposed method of column correlation requires a stronger assumption about the sources (statistical independence) than the beamformer method (statistical uncorrelatedness). However, no additional assumptions are required for the proposed method beyond what is required for applying ICA, which is increasingly being used for EEG/MEG data.

Acknowledgment: This work was partially supported by NIH grant F32-NS052048 and NIH Grant R01-DC004855.

6. REFERENCES

- [1] J.F. Cardoso, "Blind signal separation: Statistical principles," *Proc. IEEE*, Vol. 86, pp. 2009-2025, Oct. 1998.
- [2] S.S. Nagarajan, H.T. Attius, K. Sekihara, and K.E. Hild II, "Partitioned factor analysis for interference suppression and source extraction," *Independent Component Analysis and Signal Separation*, Charleston, SC, pp. 189-197, Mar. 2006.
- [3] K. Sekihara, S.S. Nagarajan, D. Poeppel, and A. Marantz, "Asymptotic SNR of scalar and vector minimum-variance beamformers for neuromagnetic source reconstruction," *IEEE Trans. on Biomedical Engineering*, Vol. 51, No. 10, pp. 1726-1734, Oct. 2004.